

Active Vibration Cancellation

R. Kashani, Ph.D.

www.deicon.com

When the disturbance is periodic and continuously excites the structure the vibration continues at steady state, mainly at the disturbing frequencies. This forced vibration attenuation problem, known as vibration absorption (or sometimes called vibration cancellation) can be addressed by introducing controlled excitation (forces/moments) to the structures, with appropriate amplitudes and phase angles, at disturbing frequencies. Feedforward, in general, and adaptive feedforward, in particular, control are widely used as vibration cancellation techniques. These methods are extensively used in active noise abatement, as well.

1 Feedforward Control

A simple single frequency feedforward controller, applied to a noise cancellation problem, is depicted in Figure 1. *FP* is the forward path between the disturbance input and the audible noise at the output.

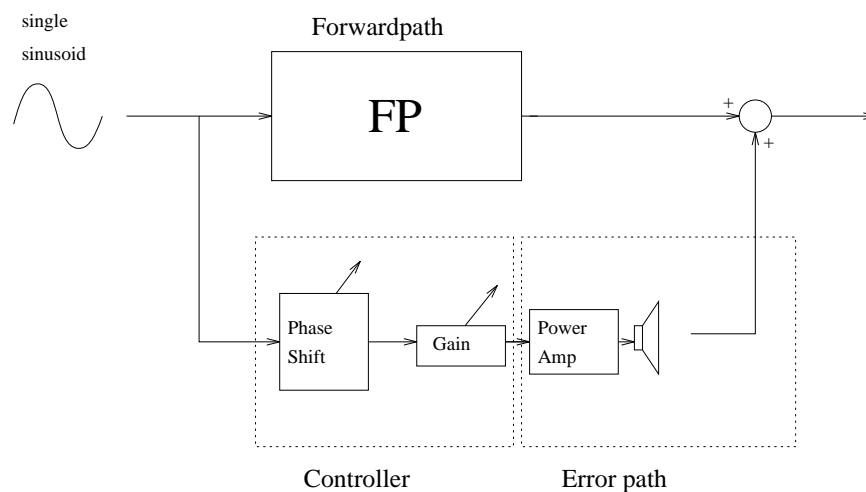


Figure 1: Single frequency feedforward controller

For a single sinusoidal input the output will also be a sinusoid at that frequency, but with an amplitude which is the input amplitude multiplied by some gain G and a phase shift ϕ . The phase shift and gain on the controller are manually adjusted until the total gain from error path and controller matches G and the total phase shift from error path and controller is 180° out of phase with ϕ . This is the basic principle of feedforward control.

The feedforward control system should cause complete cancellation of the disturbance effects at the sensor, if the gain of the controller and error path combined, matches the forward path gain exactly, and if combination of the controller and error path is exactly 180° out of phase with the forward path. When

these parameters are not exact, the cancellation will be somewhat less than perfect and in severe mismatch cases, the feedforward controller will actually worsen the system disturbance response. Considering the importance of gain and phase matching in feedforward control, it is desirable to implement some type of adaptive algorithm to minimize these errors. A least mean square (LMS) algorithm based on minimizing the mean square of the disturbance response, commonly used in noise and vibration control, will be used in this work.

2 The LMS Adaptive Feedforward Control

The essence of the LMS algorithm was presented by Widrow and Hoff in 1960. The basic concept and development of the LMS algorithm is as follows. Given the system in Figure 2, the single sinusoidal

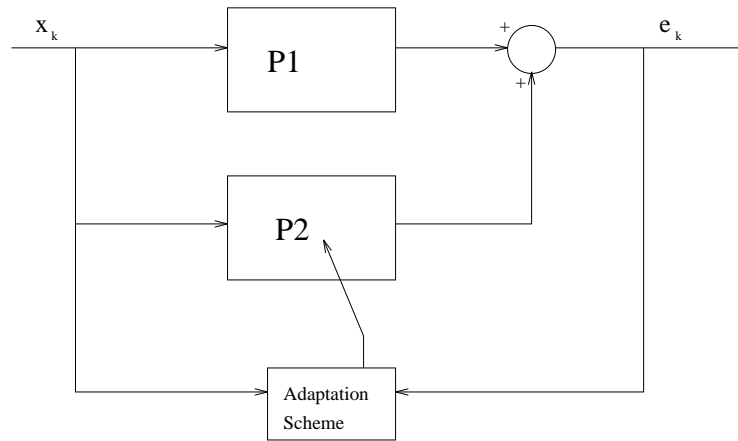


Figure 2: Basic adaptive algorithm block diagram

disturbance will pass through the plant P1 with some gain G and phase shift ϕ . It is desired to use the disturbance response signal, referred to as the error signal, $e(n)$ to adapt the controller P2 in such a way so as to minimize the error signal in a mean square sense. In order to do this the controller, which will be a simple finite impulse filter (FIR) filter, will have to have at least two coefficients to provide the desired gain and phase shift.

Typical mean square error surface vs. the two coefficients of the adaptive filter, shown in Figure 3, is a paraboloid. It can be seen that there exists only one combination of the two coefficients that yields the minimum or least mean squared error. Furthermore, for such a surface, a simple gradient decent algorithm may be used to adapt the coefficients in order to obtain this minimum. The method of steepest decent is one of the possible gradient decent algorithms, used for adaptation.

The method of steepest decent states that an iterative approach can be taken to obtain the minimum point of mean squared error, in which each coefficient (optimization variable) is updated by the following scheme

$$w_{k+1} = w_k - \mu \nabla_k \quad (1)$$

Here, w_{k+1} is the new coefficient value, w_k is the previous coefficient value, ∇_k is the gradient, and μ is the adaptation coefficient. The adaptation coefficient determines the step size used for each iteration, and must be set small enough to maintain stability of the adaptation algorithm. The gradient can be expanded in the following form

$$\nabla_k = \frac{\partial E[e^2(n)]}{\partial w_k} = -2E[e_k x_k] \quad (2)$$

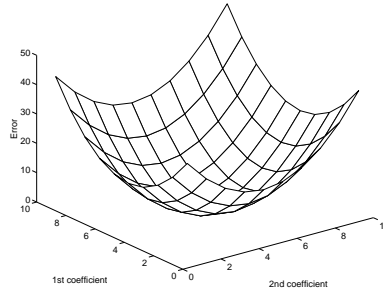


Figure 3: Typical error surface

Here, $E[\cdot]$ denotes the expectation operator, e_k is the current error signal, and x_k is the current input signal. This expression can be reduced if the assumption is made that the expected value can be replaced by the instantaneous values of the input and error. They showed that using the instantaneous values will, on average, adjust the coefficients in such a way as to reduce the mean squared error. This simplification will greatly reduce the computational need of the adaptation and make its real-time application possible.

The equation for updating the coefficients w thus becomes as follows

$$w_{k+1} = w_k + 2\mu e_k x_k \quad (3)$$

For convenience, the two, 2, is often absorbed into the adaptation coefficient μ . The block diagram for this adaptive algorithm is illustrated in Figure 4.

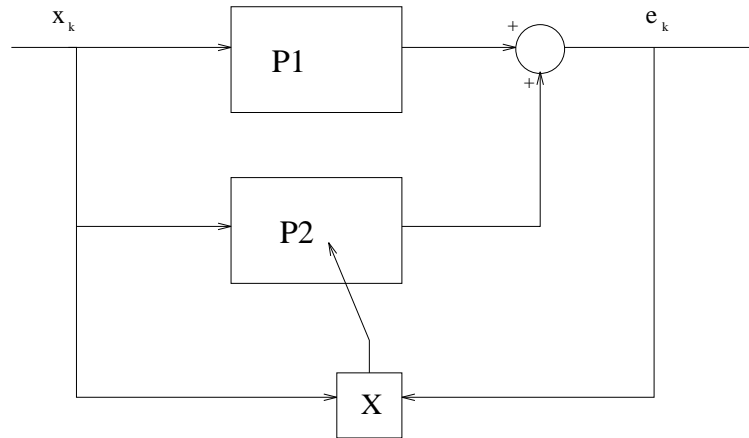


Figure 4: Basic LMS algorithm block diagram

The results of applying the LMS algorithm to an N -stage tapped delay line (TDL) filter (an N -th order FIR filter) and a sinusoidal input sampled at the rate $1/T$ were investigated by researchers. He starts with a very basic LMS algorithm as illustrated in Figure 5. The sinusoidal reference signal, resembling the disturbance, can be represented as $x_k = H \cos(\omega_r kT + \theta)$ where H is the amplitude of the reference input, ω_r is the frequency of the disturbance input, and θ is some arbitrary phase shift. Glover shows that under certain conditions the system inside the dashed box can be approximated by a linear time invariant filter $G(z)$ between e_k and y_k . The detailed derivation can be found in literature. The end result of the derivation is Equation 4 that represents the input/output relationship of the filter in the z -domain.

$$Y(z) = \underbrace{\frac{N\alpha}{4} E(z) [U(z e^{-j\omega_r T}) + U(z e^{j\omega_r T})]}_{\text{time-invariant}} + \frac{\alpha}{4} \beta(\omega_r T, N) [TV] \quad (4)$$

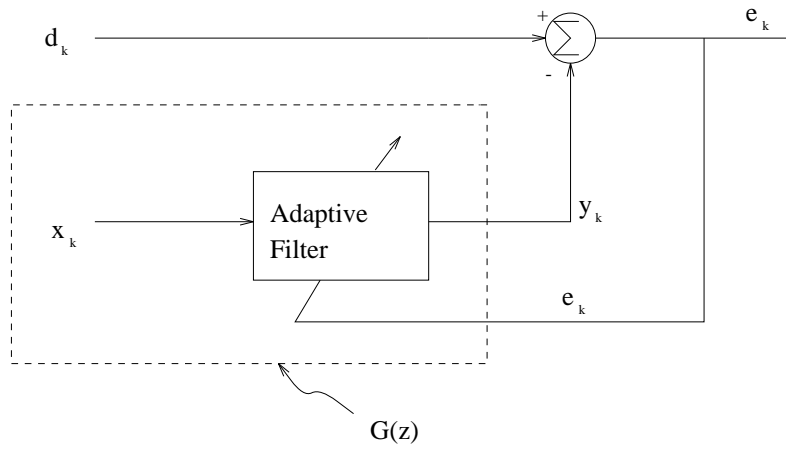


Figure 5: Glover's basic LMS algorithm

where

$$\beta(\omega_r T, N) = \frac{\sin N\omega_r T}{\sin \omega_r T},$$

$U(z) = 1/z - 1$, α is a constant, and TV represents the undesirable time-varying terms. From inspection of these equations, it is clear that reasonable measure of the relative strengths of the time variant and time invariant components of the output $Y(z)$ would be the ratio $\beta(\omega_r T, N)/N$. When this ratio is much smaller than unity, we would expect the contribution of time variant components to be insignificant compared to the time invariant components. In fact, we would prefer that $\beta/N = 0$ in which case only the time invariant components remain. The ratio β/N can be made small by either, making N large, or by selecting T in such a way as to make β exactly zero. *The second method is known as synchronous sampling.* In order for β to be exactly zero, the numerator of β must be zero, while the denominator is non-zero. Given these conditions

$$\sin(N\omega_r T) = 0 \quad (5)$$

Realizing that the term inside the sine must be an integer multiple of π yields

$$T = \frac{\pi}{N\omega_r} \quad (6)$$

which means that the sampling frequency f would be

$$f = \frac{N\omega_r}{\pi} \quad (7)$$

$$= 2Nf_r \quad (8)$$

Thus the sampling frequency must be exactly $2N$ times the reference frequency. It is for this reason that the method is known as synchronous sampling. Since N must be at least two, the sampling rate must be at least four times the reference frequency. Glover goes on to show that the frequency response of the entire system is that of a notch filter centered at the reference frequency f_r and with a bandwidth of $(N\alpha)/(2T)$ radians per second. This finite bandwidth is a result of the time varying coefficients of the adaptive filter, since a constant coefficient filter could only produce an output at the reference frequency and could not affect neighboring frequencies. This system is equivalent to using an adaptive bandpass filter as a feedback controller between $E(z)$ and $Y(z)$.

2.1 Filtered-X LMS Feedforward Control

The basic LMS algorithm could be implemented, exactly as described above, if there were no error path dynamics in the system. In practice, there are dynamics involved in the error path from the controller to the output sensor. This problem was addressed estimating of the error path be used to filter the input signal just before entering the LMS algorithm. It was found that this effectively compensates for the effect of the error path on the control signal. This method of compensation combined with the LMS algorithm later became known as the filtered-X algorithm. The stability of the filtered-X algorithm was explored by Morgan. He showed that if the adaptation coefficient μ were made small enough, the coefficients of the adaptive filter would converge to the optimal values, even with errors in the phase of the error path estimate of up to 90° . A block diagram of the filtered-X algorithm is illustrated in Figure 6.

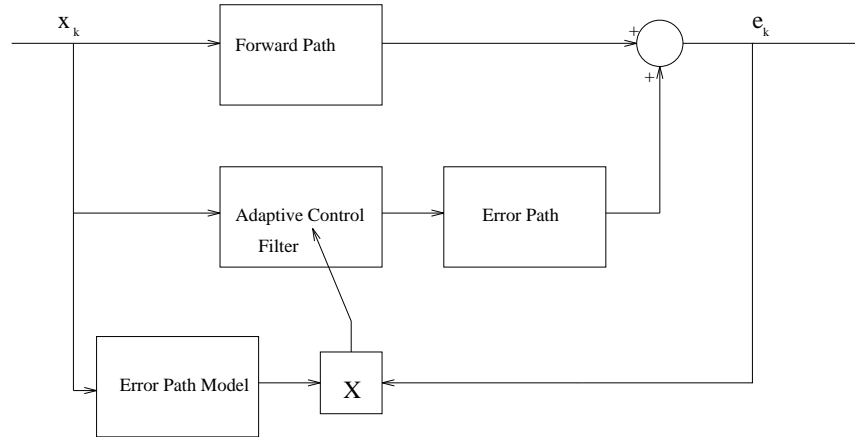


Figure 6: Block Diagram of Filtered-X System.

Although the block diagrams of 4 and 6 give the impression that the measure of disturbance, in its entirety, should be available to the controller and adaptation routine, it should be noted that only the periodicity attribute of the disturbance is measured and made available to the adaptive control scheme.

Example 2.1: Adaptive feedforward control in milling

The effectiveness of the LMS adaptive feedforward controller is illustrated by cancelling the harmful effects of cutter runout disturbance rejection in a milling process. The cutting force component in the feed direction was measured with a platform dynamometer. A piezoelectric stack actuator is used for introducing the control to the machine by manipulating the table, holding the part. A angular velocity is used, as the reference signal, for feedforward control adaptation.

Referring to Figure 6, the error path block describes the transfer function mapping the control, i.e., the table position, to the cutting force. The forward path block describes the mapping between cutter runout and the cutting force. The X block is the filtered-X LMS algorithm adapting the control filter. Error path block is a simplified model of the error path which as stated earlier can have up to 90° of phase error with the actual error path dynamics and still make the adaptation routine converge.

System identification or a simplified analytical modeling approach can be used to construct this model. A second order discrete-time model presented by a difference equation shown in Equation 9,

$$f(k) = 0.0016u(k-1) - 0.0013u(k-2) + 0.6722f(k-1) + 0.3264f(k-2) \quad (9)$$

has been identified to map the actuator force (u) to the cutting force (f). Identification has been performed cutting an ultrahigh molecular weight polyethelene with a four flute, 30° helix angle, $7/16$ " diameter end-

milling cutter. The cutting parameters used in this experimental modeling were: Radial and axial depth of cut of 0.05 and 0.6 in, respectively, feedrate of 3 in/min, spindle speed of 210 RPM, and sampling rate of 360/revolution. Note that this is the error path model, but since the purpose of this numerical example is the illustration of the mechanics of adaptive feedforward control strategy, applied to cutting processes, this second order linear model is used for forward path. The simulation of the error, i.e., the deviation of the cutting force from the desired value is shown in Figures 7, 8, and 9.

Figure 7 illustrates the effects of considering more than one harmonic of the disturbance input, using an 8 tap filter and adaptation coefficient of $\mu = 0.05$. Figure 8 shows the effects of having feedforward

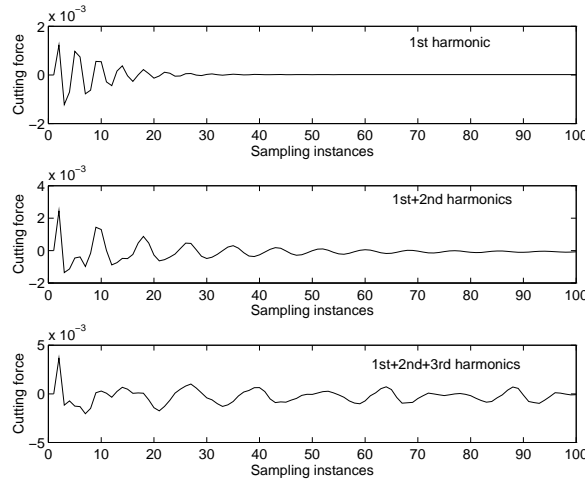


Figure 7: The effect of considering higher order harmonics of cutter runout disturbance

control filter with 2, 4, 6, and 8 taps, respectively, on the performance. All of these simulations are done with the adaptation coefficient of $\mu = 0.05$ and with two harmonics of the disturbance present. As indi-

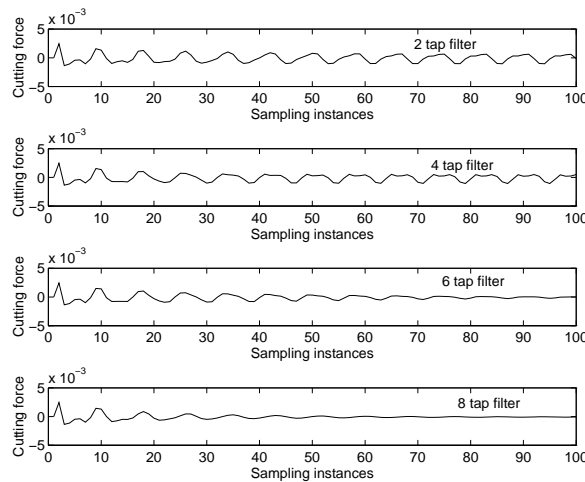


Figure 8: The effect of varying the number of taps in the controller

cated in Figure 8, the effectiveness of the controller and the rate of convergence of the adaptation increases with increasing the number of taps. The cost for using higher number of taps is more real-time computations to come up with the higher number of filter coefficients, i.e., the optimization variables. Figure 9 demonstrates the influence of the adaptation coefficient on the convergence speed of the adaptation. The

adaptation coefficients used are $\mu = .02, 0.05, 0.1,$ and 0.12 . An 8 tap controller along with two harmonics of the cutter runout disturbance input are considered for all of the adaptation coefficients used in this simulation. As the adaptation coefficient increases, the speed of convergence increases leading to higher performance in terms of disturbance rejection. As expected, too high of an adaptation coefficient, e.g. $\mu = 0.12$ in this simulation, results in instability of the controlled system.

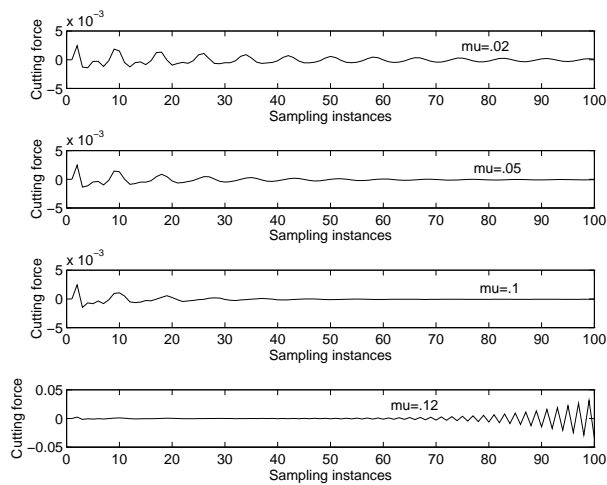


Figure 9: The effect of varying the adaptation coefficient in the controller